

Journal of Materials Chemistry B

Accepted Manuscript



This is an *Accepted Manuscript*, which has been through the Royal Society of Chemistry peer review process and has been accepted for publication.

Accepted Manuscripts are published online shortly after acceptance, before technical editing, formatting and proof reading. Using this free service, authors can make their results available to the community, in citable form, before we publish the edited article. We will replace this *Accepted Manuscript* with the edited and formatted *Advance Article* as soon as it is available.

You can find more information about *Accepted Manuscripts* in the [Information for Authors](#).

Please note that technical editing may introduce minor changes to the text and/or graphics, which may alter content. The journal's standard [Terms & Conditions](#) and the [Ethical guidelines](#) still apply. In no event shall the Royal Society of Chemistry be held responsible for any errors or omissions in this *Accepted Manuscript* or any consequences arising from the use of any information it contains.

Cite this: DOI: 10.1039/c0xx00000x

Paper

www.rsc.org/xxxxxx

Interactions of Stealth Conjugated Polymer Nanoparticles with Human Whole Blood

Raha Ahmad Khanbeigi^a, Zeina Hashim^b, Thais Fedatto Abelha^a, Simon Pitchford^a, Helen Collins^c, Mark Green^b, Lea Ann Dailey^{a*}

Received (in XXX, XXX) Xth XXXXXXXXX 20XX, Accepted Xth XXXXXXXXX 20XX

DOI: 10.1039/b000000x

Photoluminescent conjugated polymeric nanoparticles (CPNs) exhibit favourable properties as fluorescent probes due to their brightness, high photostability, tunable emission spectra and ease of surface modification. Potential cellular and clinical applications of these new diagnostic agents are easily envisioned, providing a rationale to study CPN biocompatibility. Here, stealth formulations of poly phenylene vinylene (PPV) and poly phenylene ethynylene (PPE) were manufactured and their interactions with human blood components assessed. CPNs were colloidally stable in isotonic fluids, but showed photoluminescence quenching in whole blood and plasma at levels as low as 10% supplementation. At concentrations $>150 \mu\text{g mL}^{-1}$, stealth CPNs caused $\sim 10\%$ erythrocyte haemolysis, which was likely due to unbound pegylated surfactant present in the formulation. Incubation of CPNs with both whole blood and isolated platelets showed no platelet activation, increases in platelet-monocyte aggregates or induction of platelet aggregation. Interestingly, PPE-CPN formulations inhibited adenosine diphosphate (ADP)-induced platelet aggregation in a dose-dependent manner, while PPV-CPNs did not show this effect. In conclusion, stealth CPN formulations exhibiting neutrally charged, pegylated surfaces do not stimulate platelet activation or aggregation, but may induce a low degree of haemolysis in the presence of free surfactant and can inhibit physiological mediators of platelet aggregation, such as ADP.

Introduction

Originally developed as inexpensive, synthetic alternatives to metal-based semiconductors for the manufacture of light emitting diodes and photovoltaic cells¹, luminescent conjugated polymers have only recently been investigated for their potential use in biomedical research.²⁻⁹ The high photostability and fluorescence brightness, combined with an ability to modify fluorescence emission through chemical modification to the polymer structure or through formulation strategies, are attractive features of conjugated polymers as fluorescent probes in diagnostic and theranostic applications.^{6, 10}

Conjugated polymer nanoparticles (CPNs) have been prepared from a variety of polymer classes.¹ CPN optical properties are dependent upon polymer structure, ranging from systems that emit in the blue region of the visible spectrum to infrared-emitting CPNs. This variety offers a flexible palette of photoluminescent emitters which may be used both as optical probes in basic biomedical research and possibly in future clinical applications.¹¹ It has been shown that CPN surfaces can be labelled with antibodies for targeted cell imaging or may incorporate multiple contrast agents, such as gadolinium salts or iron oxide nanoparticles, to create multifunctional diagnostic probes.²⁻⁹ Further, a handful of studies have investigated the encapsulation of therapeutic agents within a CPN matrix, demonstrating the potential for developing theranostic systems.¹¹⁻¹⁴

Biocompatibility studies of these new diagnostic agents are necessary to guide the design of optimized CPN systems towards clinical and nonclinical uses. Currently, there is little published data on CPN biocompatibility and a paucity of basic research investigating CPN interactions with whole organisms, tissues, cells or physiological fluids. Thus, the aim of this study was to investigate the interactions of two model CPN systems with

^a Institute of Pharmaceutical Science, King's College London, 150 Stamford Street, London SE1 9NH, UK.

^b Department of Physics, King's College London, Strand, London WC2R 2LS, UK

^c Division of Immunology, Infection and Inflammatory Diseases, Guy's Campus, King's College London, 16-15 Newcomen Street, London SE1 1UL, UK.

* Tel: +207-848-4780; Email: lea_ann.dailey@kcl.ac.uk

different components of human whole blood. Human whole blood is an ideal system for preliminary investigations of CPN biocompatibility, especially as future clinical applications may involve administration by injection. Whole blood is a readily accessible source of human primary cells and may be used to study the complex environment encountered upon intravenous injection of CPNs. Separation of whole blood into its constituent components also provides the opportunity to study individual mechanisms of CPN interactions with specific blood components, including platelets, leukocytes and erythrocytes and plasma proteins.

Three different stealth CPN formulations were investigated in this study (Figure 1). The first formulation (PPV-2000) was comprised of a red-emitting conjugated poly phenylene vinylene (PPV) core, which was stabilized by a surface coating of dipalmityl phosphatidylcholine (DPPC) and pegylated (2000 Da) phosphatidylethanolamine (PE-PEG₂₀₀₀) in a 2:1 weight ratio. The second formulation (PPE-2000) had a core consisting of a blue-emitting poly phenylene ethynylene polymer with the same shell components as PPV-2000. A further formulation (PPE-660) consisted of the same PPE polymer core, but was stabilized by a surface coating comprised entirely of pegylated (660 Da) 15-hydroxystearate (Solutol®). All stealth CPN systems were compared with carboxyl-modified polystyrene beads (cPS; 50 nm diameter), which have been shown in previous studies to activate human platelet cells and influence coagulation pathways due to their high negative surface charge.^{15,16}

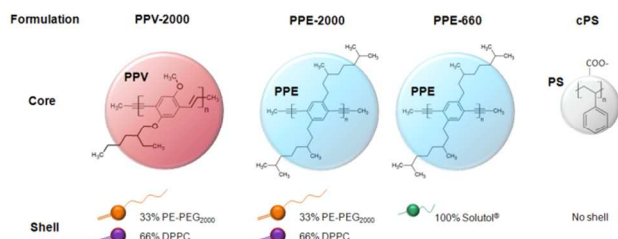


Figure 1. Diagram of the nanoparticle core-shell composition for all particles investigated in this study. From left to right: PPV-2000, PPE-2000 and PPE-660 conjugated polymer nanoparticles; plus commercially available carboxylated polystyrene beads (cPS).

Experimental Section

Materials

Poly [2,5-di(3',7'-dimethyloctyl) phenylene-1,4-ethynylene] (PPE, Mw unknown) and poly[2-methoxy-5-(2-ethylhexyloxy)-1,4-phenylenevinylene] (PPV; MW 40 – 70 kDa) were purchased from Sigma-Aldrich (Dorset, UK). Solutol® HS15 was acquired from BASF (Ludwigshafen, Germany). 1,2-dipalmitoyl-sn-glycero-3-phosphoethanolamine-N-[methoxy(polyethyleneglycol)-2000] (ammonium salt) (PE-PEG₂₀₀₀) and 1,2-dipalmitoyl-sn-glycero-3-phosphocholine (DPPC) were purchased from Avanti Lipids (Alabama, US). Carboxylated polystyrene nanoparticles with a diameter of 50 nm (2.62% m/v) were used as a reference material and were purchased from Polysciences (Eppelheim, Baden-Württemberg, Germany). All other materials were of analytical grade.

CPN fabrication

In a typical PPV-2000 or PPE-2000 preparation, 35.5 mg PE-

PEG₂₀₀₀ and 20.4 mg DPPC were dispersed in 25 mL purified water in a round-bottom flask. To ensure homogeneity of the phospholipid dispersion, the mixture was sonicated four times in a 35 kHz ultrasound water bath using ice to maintain a temperature below 7°C. Each sonication cycle lasted 60 seconds with 30 second rest periods in between. The dispersion was then magnetically stirred for 1 minute, while 0.8 mL PPV or PPE solution (3.125 mg mL⁻¹ polymer in dichloromethane; DCM) was introduced with a syringe over a period of 60 seconds. The flask was covered, stirred vigorously for 10 minutes, and sonicated for 90 seconds at 7°C. The open flask was gently stirred overnight to promote full DCM evaporation and the sample filtered through a 0.2 μm membrane filter prior to storage at 4°C. To prepare PPE-660 formulations, the same procedure was used, but the PE-PEG₂₀₀₀/DPPC mixture was replaced by a dispersion of 135 mg Solutol® in 25 mL purified water.

To remove excess surfactant, all CPN suspensions were dialyzed (Spectra/Por dialysis tubing, MWCO 300 kDa; VWR International Ltd, UK) against deionised water containing 3 g L⁻¹ Bio-Bead SM 2 Adsorbents (Bio-rad, UK). The dialysis step was repeated three times with each cycle lasting ~3, 7.5, and 10 hours, respectively. Prior to experimentation, the samples were concentrated using centrifugal filter units (Amicon Ultra, Millipore; UK; MWCO 100 kDa). Solutol® quantification was performed before (6.49 ± 1.32 mg mL⁻¹) and after (0.10 ± 0.03 mg mL⁻¹) the purification process as described by Jones et al.¹⁷, showing a removal of ~98% free surfactant. Residual PE-PEG₂₀₀₀/DPPC was not determined in this study.

CPN concentration in the final suspension was determined by drying a known volume of CPN sample and then dissolving it in a known amount of chloroform + 1% methanol. Absorbance of the sample was measured and the concentration determined using the mass extinction coefficient value of particles in chloroform + 1% methanol (PPV at 490nm, $\epsilon=74.50$ L mg⁻¹ cm⁻¹; PPE at 400 nm, $\epsilon=48.49$ L mg⁻¹ cm⁻¹).

CPN physicochemical characterisation

Nanoparticle hydrodynamic diameters (HD) were measured in pure water and 0.9% sodium chloride (NaCl) solution using both photon correlation spectroscopy (PCS; Nanosizer, Malvern Instruments, UK) and particle tracking analysis (PTA; Nanosight, UK). PCS measurements were made using a scattering angle of 173°, an estimated refractive index of particles=1.590, refractive index of water = 1.337, temperature = 25°C, and dynamic viscosity of water = 1.002 mPa s. PTA measurements were performed in water at room temperature using the following capture settings. Camera type: sCMOS, Shutter length 32.493 ms, shutter setting 130, Camera gain 512. The zeta potential was measured using the Nanosizer in 6 mM NaCl at 25°C and 6 mM NaCl containing 10% human plasma at 37°C. Zetasizer Software 6.20 was used to analyse the data.

Human blood collection and processing

Whole blood was collected in citrate buffer from healthy male and female Caucasian volunteers aged 25-45 years old with no reported medication. All donors provided consent and the study was approved by the local ethics committee. Approximately 80% of each blood sample was used to isolate erythrocytes (RBC), platelet rich plasma (PRP) and platelet poor

plasma (PPP) for use in further studies. Erythrocytes were isolated by centrifugation at 800 g for 15 min. To prepare PRP, 5 mL aliquots of whole blood were centrifuged at 100xg for 20 min and the PRP separated from the other blood components. To produce PPP, aliquots of PRP were centrifuged at 1400xg for 10 min and the PPP recovered. Whole blood, erythrocytes, PRP and PPP samples were stored at room temperature and utilized within 4 hours of collection.

CPN hydrophobicity and interactions with human plasma

Surface hydrophobicity of nanoparticle suspensions ($n=3$ individual batches) in the presence and absence of 10% human plasma (PPP) was assessed using hydrophobic interaction chromatography (HIC).¹⁷ Briefly, nanoparticle suspensions were suspended in PBS or PBS supplemented with 10% PPP ($\sim 300 \mu\text{g mL}^{-1}$) and incubated 1 h at 37°C. Non-particle bound proteins were removed by centrifugation at 13,000 rpm for 15 min, removal of the supernatant and resuspension in PBS. The washing procedure was repeated three times. Suspensions (250 μL) were then eluted through three different HiTrapTM substituted sepharose hydrophobic interaction columns: Butyl FF, Phenyl FF (high substitution) and Octyl FF (GE Healthcare Life Sciences, Little Chalfont, UK). The eluent was collected in 1 mL fractions and analyzed for particle content via turbidity measurement (SpectraMax 190, Molecular Devices, CA, USA; $\lambda=650 \text{ nm}$). Particles were subsequently eluted from the column using 0.1% Triton X-100. Absorbance values were plotted against elution volumes and two area under the curve (AUC) values were calculated using PrismTM 6.0 software (Graphpad Prism 5, CA, USA). The particle retention (%R) in each of the three columns was defined according to Equation (1):

$$(1) \% R = \left(\frac{AUC_{TritonX}}{AUC_{PBS} + AUC_{TritonX}} \right) \times 100$$

The HIC index value was calculated according to Equation (2):

$$(2) HIC \text{ Index} = \frac{(\%R_{butyl} \times 0.47) + (\%R_{phenyl} \times 0.94) + (\%R_{octyl} \times 2.05)}{(100\% \times 0.47) + (100\% \times 0.94) + (100\% \times 2.05)}$$

whereby, 0.47, 0.94 and 2.05 represent the log P values of each column linker (butyl, phenyl and octyl modified columns, respectively) as calculated using Marvin Sketch (version 5.5.0.1, Chem Axon Limited). In the denominator, each log P value was multiplied by 100%, which represents the theoretical case of 100% retention on each column achieved by a particle with maximum hydrophobicity.

CPN optical properties in whole blood and plasma

CPN luminescence was characterized in the presence of whole blood and PPP. CPNs were incubated at a concentration of 36 $\mu\text{g mL}^{-1}$ in whole blood or PPP:PBS mixtures at volume ratios of 0:100, 10:90, 25:75, 50:50 and 100:0. A Cary Eclipse fluorescence spectrophotometer (Varian, UK) was used to measure the fluorescence intensity using $\lambda_{\text{EX}}=388 \text{ nm}$ and $\lambda_{\text{EM}}=470 \text{ nm}$ for PPE formulations and $\lambda_{\text{EX}}=496 \text{ nm}$ and $\lambda_{\text{EM}}=593 \text{ nm}$ for PPV formulations.

Assessment of erythrocyte haemolysis

CPNs were investigated for their ability to induce erythrocyte haemolysis using a colorimetric assay developed by Dobrovolskaia et al (2008).¹⁸ Briefly, a haemoglobin standard curve was prepared by diluting the haemoglobin standard in cyanmethaemoglobin (CMH) reagent (Stanbio Laboratory, Boerne, TX, USA) in the range of 25-800 $\mu\text{g mL}^{-1}$. A 40% solution of PEG (8 kDa) in water was prepared as the negative control and 1% Triton-X 100 in water was used as a positive control.

Whole blood was collected from three different donors and pooled. Haemoglobin concentration of the pooled whole blood sample was determined by mixing 100 μL whole blood with 100 μL CMH reagent in a 96-well plate, shaking for 1-2 minutes and measuring the absorbance at 540 nm. Using the calibration curve, concentration of haemoglobin in the pooled blood was calculated and the concentration adjusted as necessary by dilution with $\text{Ca}^{2+}/\text{Mg}^{2+}$ -free Dulbecco's phosphate buffered saline (DPBS) to $10 \pm 2 \text{ mg mL}^{-1}$ total haemoglobin.

Erythrocyte haemolysis was determined by diluting 100 μL test samples, blanks, positive or negative controls in 700 μL of DPBS and adding 100 μL whole blood ($10 \pm 2 \text{ mg mL}^{-1}$ total haemoglobin). The mixtures were incubated under agitation at 37°C for 3 h and centrifuged for 15 min at 800xg to remove undamaged erythrocytes. Aliquots of the supernatant (100 μL) from samples, blanks controls and the calibration curve were mixed with 100 μL CMH reagent in a 96-well plate, shaken for 2-3 minutes and the absorbance measured at 540 nm. Haemoglobin concentrations were calculated from the calibration curves and the results expressed as percentage haemolysis compared to the positive control (1% Triton X100). Treatment groups included: cPS (3, 30, 300 $\mu\text{g mL}^{-1}$), PPV-2000 (3, 30, 300 $\mu\text{g mL}^{-1}$), PPE-2000 ((3, 30, 250 $\mu\text{g mL}^{-1}$), PPE-660 (3, 30, 180 $\mu\text{g mL}^{-1}$), Solutol[®] (0.37-750 $\mu\text{g mL}^{-1}$), PE-PEG₂₀₀₀ and DPPC (0.16-650 $\mu\text{g mL}^{-1}$).

Assessment of platelet activation in isolated platelets

PRP of four donors was isolated as described above and diluted to a concentration of $10^7 \text{ cells mL}^{-1}$ in PBS containing 1% bovine serum albumin (BSA) and 0.1% sodium azide. Platelets (100 μL) were allowed to recover at room temperature for 45 minutes prior to addition of 12 μL nanoparticle suspension achieving a final concentration of 300 $\mu\text{g mL}^{-1}$ CPNs. 0.9% saline was used as a negative control and cPS (300 $\mu\text{g mL}^{-1}$) was used as a positive control. After 5 min of incubation, platelets were fixed with 100 μL PBS containing 1% BSA, 0.5% paraformaldehyde and 0.1% sodium azide, then sedimented via centrifugation (1400xg for 10 min), resuspended in 100 μL PBS containing 1% BSA and 0.1% sodium azide, and separated into two 50 μL aliquots. One aliquot (control) was mixed with 1.25 μL mouse anti-human CD41a-FITC conjugate (fluorescein isothiocyanate; $\lambda_{\text{EX}}=488 \text{ nm}$, $\lambda_{\text{EM}}=520 \text{ nm}$; BD Biosciences). The second aliquot (sample) was mixed with 1.25 μL mouse anti-human CD41a-FITC conjugate and 1.25 μL mouse anti-human CD62P-PE conjugate (R-phycoerythrin; $\lambda_{\text{EX}}=496 \text{ nm}$, $\lambda_{\text{EM}}=578 \text{ nm}$; BD Biosciences). Isotype controls were conducted for both antibodies. Following 20 minutes incubation under light exclusion at room temperature, 500 μL PBS containing 1% BSA and 0.1% sodium azide was added to the samples. Platelet activation was measured using a Cyto500 flow cytometer (BD

Biosciences). Platelets were discriminated from free particles by setting the forward scatter to 10% (side scatter 0%) and gating for CD41a+ events (threshold fluorescence intensity >1 arbitrary units). 10,000 CD41a+ events were counted for each sample and the fluorescence intensity (FI) of the FITC-marker was plotted against the FI of the CD62P (PE)-marker. The percentage CD41a+/CD62P+ events from control experiments were subtracted from the percentage of CD41a+/CD62P+ events from each sample prior to reporting results from n=4 separate donors.

10 Assessment of platelet adhesion to monocytes in whole blood

Whole blood (100 μ L) was mixed with 12 μ L CPNs or cPS achieving a final concentration of 300 μ g mL⁻¹ nanoparticles. 0.9% saline was used as a negative control. Following 5 min of incubation, samples were separated into two 50 μ L aliquots. One aliquot (control) was mixed with 1.25 μ L mouse anti-human CD14-PE-Cy7 conjugate (fluorescein isothiocyanate; λ_{ex} =488 nm, λ_{em} =520 nm; BD Biosciences). The second aliquot (sample) was mixed with 1.25 μ L mouse anti-human CD14-PE-Cy7 conjugate and 1.25 μ L mouse anti-human CD41a-FITC conjugate. Isotype controls were conducted for both antibodies. Following 20 minutes incubation under light exclusion at room temperature, 500 μ L Optilyse[®] solution was added to controls and samples. Using a forward scatter of 100% (side scatter 0%), the flow cytometer was set to gate for CD14+ events (threshold fluorescence intensity >1 arbitrary units). 3,000 CD14+ events were counted for each sample and the fluorescence intensity (FI) of the PE-Cy7-marker was plotted against the FI of the CD41a (FITC)-marker. The percentage CD14+/CD41a+ events from control experiments were subtracted from the percentage of CD14+/CD41a+ events from each sample prior to reporting results from n=4 separate donors.

Assessment of platelet aggregation in isolated platelet studies

Platelet rich plasma (PRP) and platelet poor plasma (PPP) of four healthy human volunteers were collected and processed as previously described. The concentrations of platelets in the PRP were adjusted to 2.6×10^8 platelets mL⁻¹ using PPP from the same donor. To determine whether the presence of nanoparticles will induce aggregation in isolated platelets a PAP-4 Bio-Data Corporation Platelet Aggregometer was calibrated to 100% aggregation using PPP and 0% aggregation using PRP from each individual donor. Nanoparticle suspensions (25 μ L) or 0.9% saline solution as the negative control were mixed with 225 μ L PRP (final nanoparticle concentrations tested were 3, 30 and 300 μ g mL⁻¹) and turbidity was monitored for 5 minutes at 37°C under constant stirring. Subsequently, 6 μ L adenosine diphosphate (ADP; final concentration: 10 μ M) were added to induce platelet aggregation and turbidity was monitored for a further 5 minutes. Platelet aggregation was monitored over time until a plateau was reached and this value was considered the final percentage aggregation value.

Statistical analysis

Statistical comparisons were conducted using Graph Pad Prism (San Diego, CA). $p < 0.05$ were considered significant: * <0.05 , ** <0.01 , *** <0.001

55 Results

CPN characterisation

Stealth CPNs prepared by an emulsification-precipitation method produced narrowly dispersed nanoparticles with hydrodynamic diameters of approximately 180 nm (Table 1). In water they were observed to be colloiddally stable over storage periods exceeding several months. Incubation in isotonic saline (treatment vehicle) over 1 h showed evidence of mild CPN aggregation with hydrodynamic diameter values increasing approximately 10-20%. No evidence of aggregation of cPS was observed over this time period. The observation of mild CPN aggregation in isotonic saline (150 mM) was unexpected, since particle stabilisation with non-ionic surfactants is usually less sensitive to changes in the ionic strength of suspension media, compared to particles stabilized by charged surfaces or surfactant stabilizers.¹⁹

The zeta potential of the three pegylated CPN formulations was neutral to slightly negative, as expected for colloidal systems stabilised with non-ionic surfactants (Table 1). cPS exhibited a highly negative zeta potential, also as expected. In diluted human plasma, it could be seen that the surface charge was neutralized for all nanoparticle types, indicating a significant adsorption of plasma components, such as proteins, to the cPS surface and also possibly a minor degree of protein adsorption to the CPN surfaces.

80 Table 1. Hydrodynamic diameters (HD; nm) and zeta potential (ZP; mV) values of nanoparticles in different media. Values represent the mean \pm standard deviation of n=3 measurements.

		PPV-2000	PPE-2000	PPE-660	cPS
HD (nm)	H ₂ O	145 (± 3)	181 (± 10)	190 (± 18)	49 (± 2)
	150 mM NaCl	179 (± 6)	202 (± 12)	237 (± 14)	46 (± 4)
ZP (mV)	6 mM NaCl	-12.8 (± 2.0)	-10.8 (± 0.8)	-12.9 (± 0.4)	-40.5 (± 4.2)
	6 mM NaCl + 10% plasma	-10.7 (± 0.2)	-6.0 (± 0.6)	-6.9 (± 0.9)	-6.7 (± 0.5)

Plasma protein interactions with the particle surface were also investigated indirectly using HIC and the calculated HIC index value (Figure 2). The HIC index is a purpose-developed, quantitative scaling system for nanoparticle hydrophobicity with a value of 0.00 denoting minimum hydrophobicity and a value of 1.00 denoting maximum hydrophobicity.¹⁷ It has been previously used to investigate the relationship between nanoparticle surface hydrophobicity and biocompatibility, whereby it was demonstrated that nanomaterials with exposed highly hydrophobic surfaces caused induced acute inflammation following pulmonary administration.^{17,20}

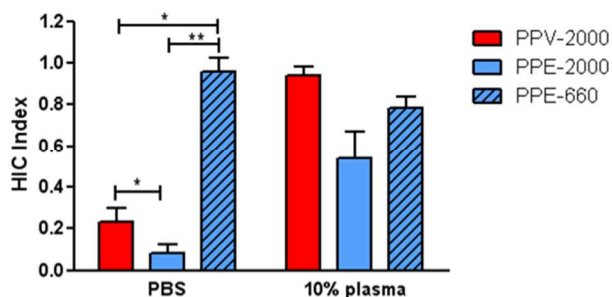


Figure 2. HIC index values for CPNs following incubation in either PBS or PBS supplemented with 10% human plasma. HIC values represent the mean \pm standard deviation of $n=3$ measurements. * $p<0.05$; ** $p<0.01$.

It was hypothesized that the pegylated surfactants would effectively shield the hydrophobic polymer core of the CPNs, thus preventing column retention of the nanoparticles and resulting in a low HIC index value. Both PPV-2000 and PPE-2000 exhibited a low HIC index score (<0.3), indicating that the pegylated phospholipids were highly effective at shielding the particle core from the hydrophobic column material, even after a rigorous washing procedure to remove excess surfactant. In contrast, PPE-660 formulations showed a high retention in the three HIC columns, resulting in an HIC index value of 0.96 ± 0.06 , which is very similar to the values measured for unmodified polystyrene beads reported previously.¹⁷ We have also observed a similar HIC index value (~ 0.96) for Solutol[®]-coated polyfluorene-based CPNs (data not shown). Solutol[®] was chosen as a CPN stabilizer as it was an inexpensive alternative to pegylated phospholipids and is further a 'generally regarded as safe' (GRAS) excipient approved for intravenous use. Its hydroxyl group at position 12 on the fatty acid chain may be responsible for reducing the strength of the hydrophobic interactions between the fatty acid chain and the hydrophobic polymer core, leading to a lower affinity of the surfactant to the hydrophobic particle surface. There is very little information reported in the literature about its adsorption affinities to solid surfaces as the surfactant is primarily used in liquids as a micelle-forming agent for drug solubilization³⁹.

Incubation of nanoparticle suspensions in PBS + 10% human plasma resulted in substantially higher HIC index values for PPV-2000 and PPE-2000, while PPE-660 exhibited a slight decrease in HIC index score. This change to the HIC index score indicates that the CPN surface was modified by the presence of plasma proteins, creating a new surface which was more hydrophobic than the original pegylated surface, but less hydrophobic than the polymer core. Overall, the HIC assay reveals that the DPPC: PE-PEG₂₀₀₀ coating provides a sufficiently extensive coverage of the polymer core (regardless of conjugated polymer used) to prevent interactions with the HIC column, but incubation with serum proteins can displace these phospholipid surfactants from the particle surface. The Solutol[®] coating showed a lower affinity to the polymer core of the nanoparticle, both in the presence and absence of proteins.

The optical properties of the stealth CPNs were investigated in the presence of human whole blood or plasma (Figure 3). Fluorescence intensity of the different formulations was measured in PBS:plasma or PBS:whole blood mixtures at

different ratios. Differences were observed between PPV and PPE formulations, whereby PPV fluorescence intensity decreased with increasing concentrations of plasma and was wholly undetectable in whole blood. In contrast, the presence of as little as 10% plasma and whole blood caused a reduction in PPE fluorescence intensity to ~ 70 -80%, however further quenching did not occur at higher concentrations of these biofluids. No significant differences were observed between PPE-2000 and PPE-660, indicating that surfactant composition did not affect optical properties.

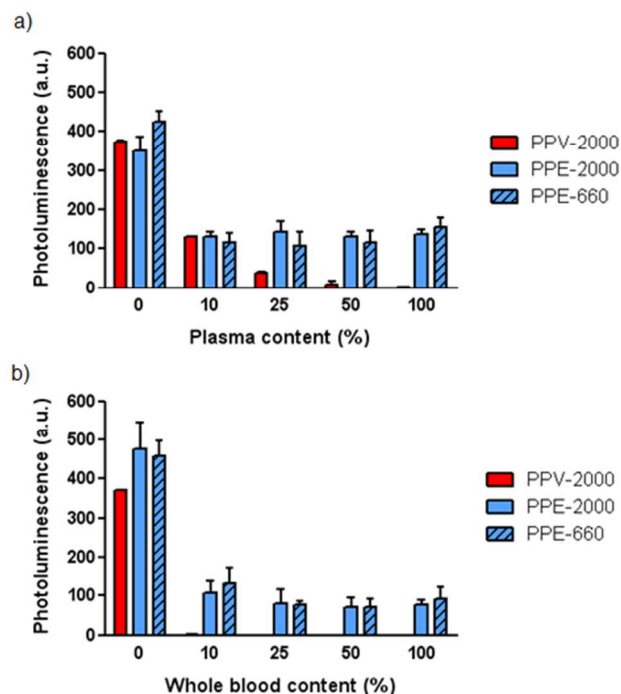


Figure 3. Photoluminescence intensity of CPN formulations ($36 \mu\text{g mL}^{-1}$) in mixtures of (a) PBS:plasma or (b) PBS: whole blood. Values represent the mean \pm standard deviation of $n=4$ independent experiments. All photoluminescence values from samples diluted in 10-100% plasma or whole blood:PBS mixtures were significantly ($p<0.001$) lower than the corresponding values of nanosuspensions diluted in PBS alone.

CPN interactions with cellular components of human blood

The haemolytic activity of the nanoparticles and surfactants was studied. Anionic cPS beads showed no erythrocyte haemolysis at concentrations up to $300 \mu\text{g mL}^{-1}$, while pegylated formulations showed increases in haemolytic activity up to $\sim 25\%$ at the highest concentrations tested. The haemolysis activity is a relative value, but many studies set 10% haemolysis as the cut off point for toxicity.^{21,22} It is difficult to compare haemolysis results across the literature due to the different incubation times and methods used in most of the haemolysis assays.¹⁸ However, it is possible that the elevated haemolysis activity at high CPN concentrations was due to the displacement of surfactant from the CPN surface by serum proteins, as seen occurring in the HIC experiments. Low levels of unbound surfactant which could not be removed during the rigorous purification process may have also contributed to this effect. The haemolytic activity of the surfactants used was also measured and the free surfactants

demonstrated haemolytic activity across a wide range of concentrations, with PE-PEG₂₀₀₀ showing the highest activity (Figure 4b).

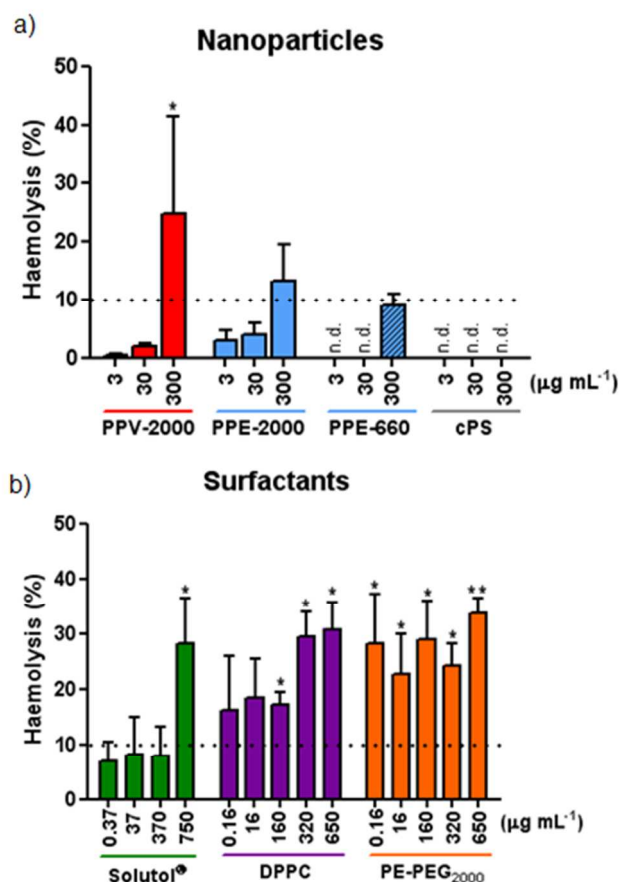


Figure 4. a) Assessment of the haemolytic potential of PPV-2000, PPE-2000, PPE-660 and cPS (3, 30, 300 µg mL⁻¹). b) Assessment of the haemolytic potential of the three surfactants, PE-PEG₂₀₀₀, DPPC, and Solutol® over a concentration range of 0.2-750 µg mL⁻¹. Values represent the mean ± standard deviation of n=3 independent experiments.

Haemolysis values significantly higher than 10% are denoted as follows: * p<0.05; ** p<0.01.

Effects of CPNs and cPS were studied on whole blood and isolated platelets. The ability of nanomaterials to activate platelets has been studied extensively using upregulation of P-selectin as an activation marker as well as the adhesion of activated platelets to monocytes.^{15,16,23,24} In this study, only PPE-CPNs were investigated, as the fluorescence emission of the PPV polymer overlapped with the fluorescence profile of the conjugated antibodies used to identify cell activation markers and even small amounts of cell-associated PPV-2000 CPNs prevented robust antibody detection during flow cytometry (Figure S1, supplementary data). Incubation of isolated platelets with cPS nanoparticles resulted in a significant stimulation of platelet activation as observed through P-selectin upregulation and surface expression (Figure 5a) and also stimulated in a significant increase in the number of platelet-monocyte aggregates detected in whole blood following cPS incubation (Figure 5b). In contrast, both PPE-CPN formulations showed no platelet activation or

significant increase in platelet-monocyte aggregates compared to the vehicle control. Finally, it should also be noted that a small control study was performed in a single donor, showing no effects of treatment with 0.9% NaCl containing either Solutol® (50-200 µg mL⁻¹) or PE-PEG₂₀₀₀/DPPC mixture (50-200 µg mL⁻¹; data not shown), indicating that the presence of residual free surfactants did not influence the study results.

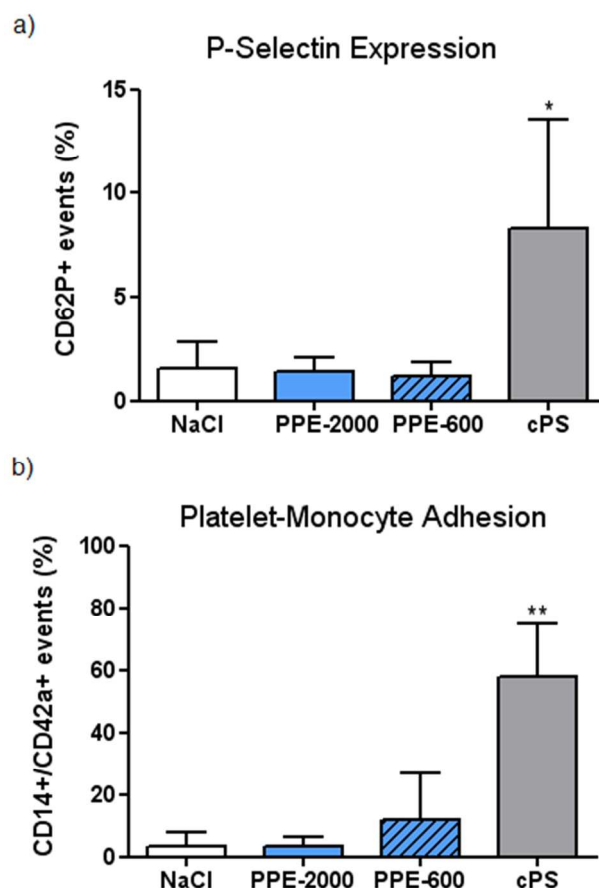


Figure 5. a) P-selectin expression in isolated platelets following 5 min incubation with vehicle control (0.9% NaCl), PPE-2000, PPE-660 and cPS nanoparticles (300 µg mL⁻¹). b) Platelet-monocyte aggregates in whole blood following 5 min incubation with vehicle control (0.9% NaCl), PPE-2000, PPE-660 and cPS nanoparticles (300 µg mL⁻¹). Values represent the mean ± standard deviation of n=4 independent experiments using blood from four different healthy donors. Difference to vehicle control: * p<0.05; ** p<0.01.

The ability of CPNs and cPS to directly induce platelet aggregation or alter physiologically induced platelet aggregation was subsequently tested in isolated platelets (Figure 6). Representative raw traces of the platelet aggregation experiment from one blood donor are depicted in Figure 6a-d. The traces show that all nanomaterials did not cause direct platelet aggregation over an incubation period of 5 min. Following this, ADP (10 µM) was added to each mixture to determine whether the presence of the nanoparticles influenced physiologically stimulated platelet aggregation. It was interesting to note that cPS did not cause platelet aggregation or influence ADP-induced aggregation, despite stimulating platelet activation and increased

numbers of platelet-monocyte aggregates in previous experiments. In contrast, both PPE-CPNs were observed to inhibit ADP-induced platelet aggregation in a dose-dependent manner, regardless of the type of pegylated surfactant used (Figure 6e). At the highest PPE-CPN concentration test ($300 \mu\text{g mL}^{-1}$) the presence of PPE-CPNs completely abolished the effects of ADP. Control experiments in one donor revealed that 0.9% NaCl containing either Solutol[®] or PE-PEG₂₀₀₀/DPPC mixture ($50\text{-}200 \mu\text{g mL}^{-1}$) did not behave differently to 0.9% NaCl alone (data not shown). The control experiments served to highlight that the inhibition of ADP-induced platelet aggregation was more likely to be a result of nanoparticle-platelet interactions, rather than effects of free surfactant in the system.

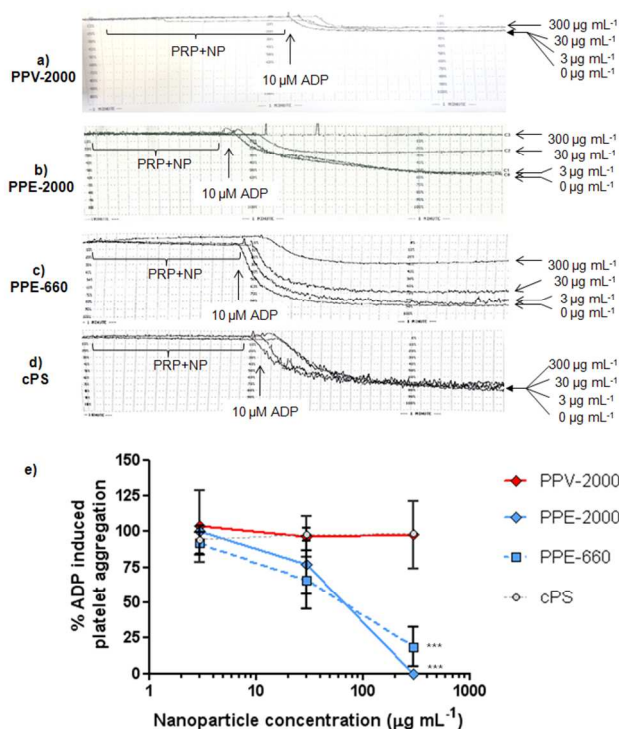


Figure 6. Effects of nanoparticle incubation on isolated platelets and ADP-induced platelet aggregation. Representative traces from single blood donors are shown. (a) PPV-2000, (b) PPE-2000, (c) PPE-660 and (d) cPS (0, 3, 30, $300 \mu\text{g mL}^{-1}$) were incubated with platelets for 5 min followed by addition of $10 \mu\text{M}$ ADP. (e) Effects of nanoparticles on ADP-induced platelet aggregation from $n=4$ donors. Difference to vehicle controls: *** $p < 0.001$.

Discussion

CPNs are currently being tested for a variety of diagnostic and theranostic applications, such as photoacoustic deep tissue molecular imaging probes, doxorubicin-loaded cancer diagnostic particles, and in photodynamic therapies.^{2,11,12,25,26} Since many of these applications involve intravenous administration of various CPN formulations, it is important to understand how the core-shell chemistry of CPNs will influence their safety and efficacy profiles following administration.

The optical properties of the CPN systems evaluated in this study were influenced by different biological environments and

modes of measurement. For example, incubation of CPN in human plasma and whole blood showed that even low concentrations of proteins added to a CPN suspension may quench the fluorescence signal measured in a fluorescence spectrophotometer, although they may be detected by a flow cytometer (supplementary information, Figure S2). This indicates that further research would be useful to outline the application-specific strengths and limitations of these systems as optical probes. Within the field of biosensor development, non-specific, protein-induced quenching of conjugated polymer fluorescence is a well-known phenomenon and has been challenging to overcome.²⁷⁻²⁹ Quenching is thought to occur through disruption to the electron mobility in the π -conjugated double-bond system of the polymers caused by direct protein interactions with the polymer chains.²⁷ For applications in biomedical imaging, CPN optical properties may be better conserved in biological environments through prevention of protein binding to the conjugated polymer core of the nanoparticles.

It was originally hypothesized that surface coating of the CPNs with a non-ionic pegylated surfactant would provide a steric barrier to prevent protein adsorption to the CPN surface. The HIC method was employed in this study to ascertain whether incubation of CPN systems with human plasma would result in changes to the particle surface through protein binding. The results revealed that PPV-2000 and PPE-2000 exhibited significantly lower HIC index values compared with PPE-660, demonstrating that PE-PEG₂₀₀₀ is better than Solutol[®] at preventing interactions between the polymer core and the column material. Interestingly, upon incubation with human plasma the HIC index values of PPV-2000 and PPE-2000 increased significantly, indicating that protein adsorption had generated a new, more hydrophobic CPN surface with potentially altered optical and biological properties.

The second aim of the study was to investigate the biocompatibility profile of CPNs using human blood as a model system. Previous studies have demonstrated that many engineered nanomaterials have undesired effects on individual blood components as well as physiological functions, such as the coagulation pathway.³⁰ For example, single and multi-walled carbon nanotubes, aminated and carboxylated polystyrene beads, nanoscale silica, carbon black, and diesel exhaust particulates can exert haemolytic activity, activate blood platelets and induce platelet aggregation.^{15,16,23,24,31-34} These parameters have also been investigated following exposure to a variety of nanomedicines, including but not limited to dendrimers, polymer, metal and ceramic nanoparticles, liposomes, quantum dots, and nanoemulsions.^{18, 30, 35-38}

The neutrally charged stealth CPN systems studied here were designed to avoid haemolysis, platelet activation, aggregation and agonist-induced aggregation in order to increase clinical feasibility. The results of this study show that some system optimisation is necessary for future clinical use. For example, all CPN formulations studied caused unacceptably high levels of haemolysis at the higher concentrations tested. Due to a lack of high-density anionic or cationic surface charge,^{15,16,30,37} the haemolytic activity is likely to result from displaced, unbound surfactant present in the system. Thus, further optimisation is

required to find surfactants with a higher affinity to the nanoparticle core material. Also, optimisation of the CPN shell composition may also reduce protein corona formation and quenching of CPN photoluminescence.

Finally, the propensity of certain CPNs, such as the PPE-based systems, to inhibit agonist-induced coagulation pathways must be further investigated. This phenomenon has been observed with other biomaterial nanoparticulate systems, notably with poly (lactic-co-glycolic acid) (PLGA), chitosan and PLGA-chitosan nanoparticles.³⁶ Li et al.³⁶ observed that these nanomaterials exerted dose-dependent inhibition of collagen-induced platelet aggregation at dose between 10-100 $\mu\text{g mL}^{-1}$, similar to the relevant dose range examined in this study. Despite the differences in core-shell chemistry between PLGA/chitosan systems and the PPE-CPNs, the observed behaviour of these nanomaterials with regard to platelet compatibility is surprisingly similar. Future studies will probe whether the extent of pegylated surfactant displacement from the particle differs significantly in 100% serum (compared to 10% serum:90% PBS, as assessed in the HIC assay), as this may influence nanoparticle attachment to the platelet surface under the conditions prevailing in the platelet aggregation assay. Secondly, it would be interesting to study whether major differences exist in the composition of the protein corona on the PPE vs the PPV nanoparticle surface and whether these differences influence CPN attachment to platelets resulting in steric hindrance of aggregation.

Conclusions

The results of this study provide useful insights to guide the future design of clinically relevant diagnostic and theranostic agents which exploit the exciting and advantageous properties of conjugated polymers. First, it was demonstrated that nanoparticle core-shell chemistry determines CPN performance in human blood. For example, both non-ionic pegylated surfactants used to coat the PPE and PPV CPN did not prevent protein adsorption to the CPN surface, thereby leading to CPN quenching and *in situ* formation of a new particle surface capable of interacting with different blood components. Secondly, all CPNs investigated demonstrated >10% haemolysis at high concentrations, which must be improved through an optimised choice of surfactant. Thirdly, PPE-CPN systems induced a dose-dependent inhibition of agonist-induced platelet aggregation, while PPV-CPNs did not. The reason for this discrepancy is currently unclear, but provides a clear rationale for further study investigating a wider range of CPN systems and their impacts on the coagulation pathway.

Acknowledgements

The authors would like to the BBSRC (UK) and the Science Without Borders programme (Brazil) for the funding of this project.

[†]Electronic Supplementary Information (ESI) available: [details of any supplementary information available should be included here]. See DOI: 10.1039/b000000x/

References

- 1 A.J. Heeger, N.S. Sariciftci, E.B. Namdas Semiconducting and metallic polymers. Oxford: Oxford University Press; 2010.
- 2 K.Y. Pu, A.J. Shuhendler, J.V. Jokerst, J.G. Mei, S.S. Gambhir, Z.N. Bao, et al. *Nat Nanotechnol.* 2014, **9**,233.
- 3 K.Y. Pu, A.J. Shuhendler, J.H. Rao, *Angew Chem Int Edit.* 2013,**52**,10325.
- 4 J.B. Yu, C.F. Wu, X.J. Zhang, F.M. Ye, M.E. Gallina, Y. Rong et al. *Adv Mater.* 2012,**24**,3498.
- 5 Y.H. Chan, C.F. Wu, F.M. Ye, Y.H. Jin, P.B. Smith, D.T. Chiu DT, *Anal Chem.* 2011,**83**,1448.
- 6 C.F. Wu, T. Schneider, M. Zeigler, J.B. Yu, P.G. Schiro, D.R. Burnham, et al., *J Am Chem Soc.* 2010,**132**,15410.
- 7 P. Howes, M. Green, J. Levitt, K. Suhling, M. Hughes, *J Am Chem Soc.* 2010,**132**,3989.
- 8 P. Howes, M. Green, *Photoch Photobio Sci.* 2010,**9**,1159.
- 9 Z. Hashim, P. Howes, M. Green, *J Mater Chem.* 2011,**21**,1797.
- 10 Y. Rong, C.F. Wu, J.B. Yu, X.J. Zhang, F.M. Ye, M. Zeigler, et al., *ACS Nano.* 2013,**7**,376.
- 11 R. Tang and X. Feng, *Canadian Chemical Transactions.* 2013,**1**,78.
- 12 X. Feng, F. Lv, L. Liu, H. Tang, C. Xing, Q. Yang, et al., *ACS Appl Mater Interfaces.* 2010,**2**,2429.
- 13 J.H. Moon, E. Mendez, Y. Kim, A. Kaur, *Chem Commun (Camb).* 2011,**47**,8370.
- 14 A.T. Silva, A. Nguyen, C. Ye, J. Verchot, J.H. Moon, *BMC Plant Biol.* 2010,**10**,291.
- 15 C. McGuinness, R. Duffin, S. Brown, N.L. Mills, I.L. Megson, W. MacNee, et al., *Toxicol Sci.* 2011,119,359.
- 16 K. Donaldson, C. McGuinness, L. Tran, V. Stone, R. Duffin, *J Phys Conf Ser.* 2009,151.
- 17 M.C. Jones, S.A. Jones, Y. Riffo-Vasquez, D. Spina, E. Hoffman, A. Morgan, et al. *J Controlled Release* 2014,183,94.
- 18 M.A. Dobrovolskaia, P. Aggarwal, J.B. Hall, S.E. McNeil. *Mol Pharmaceut.* 2008,**5**,487.
- 19 A. Watanabe. *Bull Inst Chem Res Kyoto Univ.* 1960,**38**,158.
- 20 L.A. Dailey, R. Hernandez-Prieto, A.M. Casas-Ferreira, M.C. Jones, Y. Riffo-Vasquez, E. Rodriguez-Gonzalo, et al. *Nanotoxicol.* 2014, 2014 Mar 12. [Epub ahead of print].
- 21 J.F. Bermejo, P. Ortega, L. Chonco, R. Eritja, R. Samaniego, M. Mullner, et al., *Chem-Eur J.* 2007,**13**,483.
- 22 D. Fischer, Y.X. Li, B. Ahlemeyer, J. Kriegelstein, T. Kissel, *Biomaterials.* 2003,**24**,1121.
- 23 X.Z. Wang, Y. Yang, R.F. Li, C. McGuinness, J. Adamson, I.L. Megson, et al. *Nanotoxicol.* 2014,**8**,465.
- 24 A. Solomon, E. Smyth, N. Mitha, S. Pitchford, A. Vydyanath, P.K. Luther, et al *J Thromb Haemost.* 2013,**11**,325.
- 25 D.K. Chatterjee, L.S. Fong, Y. Zhang, *Adv Drug Deliver Rev.* 2008,**60**,1627.
- 26 H. Kim, S. Mun, Y. Choi, *J Mater Chem B.* 2013,**1**,429.
- 27 C.H. Fan, K.W. Plaxco, A.J. Heeger. *J Am Chem Soc.* 2002,**124**,5642.
- 28 A. Herland, O. Inganas, *Macromol Rapid Comm.* 2007,**28**,1703.
- 29 S.W. Thomas, G.D. Joly, T.M. Swager, *Chem Rev.* 2007,**107**,1339.
- 30 A.N. Ilinskaya, M.A. Dobrovolskaia MA, *Nanomedicine.* 2013,**8**,969.
- 31 M. Forestier, M. Al-Tamimi, E.E. Gardiner, C. Hermann, S.C. Meyer, J.H. Beer. *Toxicol in Vitro.* 2012,**26**,930.
- 32 A. Radomski, P. Jurasz, D. Alonso-Escolano, M. Drews, M. Morandi, T. Malinski, et al., *Brit J Pharmacol.* 2005,**146**,882.
- 33 A. Nemmar, S. Al-Salam, S. Zia, S. Dhanasekaran, M. Shudadevi, B.H. Ali, *Toxicol Lett.* 2010,194,58.
- 34 C. Oslakovic, T. Cedervall, S. Linse, B. Dahlback, *Nanomed-Nanotechnol.* 2012,**8**,981.
- 35 A.N. Ilinskaya, M.A. Dobrovolskaia, *Nanomedicine.* 2013,**8**,773.
- 36 X. Li, A. Radomski, O.I. Corrigan, L. Tajber, F.D. Menezes, S. Endter, et al. *Nanomedicine.* 2009,**4**,735.

-
- 37 M.A. Dobrovolskaia, A.K. Patri, J. Simak, J.B. Hall, J. Semberova, S.H.D.P. Lacerda, et al., *Mol Pharmaceut.* 2012,**9**,382.
- 38 J.M. Koziara, J.J. Oh, W.S. Akers, S.P. Ferraris, R.J. Mumper,
5 *Pharm Res.* 2005,**22**,1821.
- 39 K. Buszello, S. Harnisch, R. H. Müller, B. W. Müller, *Eur. J. Pharm. Biopharm.* 2000, **49**, 143.